Combination of electrochemical biosensor and textile threads: A microfluidic device for phenol determination in tap water

F.R. Caetano[a], E.A. Carneiro[a], D. Agustini[a], L.C.S. Figueiredo-Filho[b], C.E. Banks[c], M.F. Bergamini[a], L.H. Marcolino-Junior[a,□]

[a] *Laboratório de Sensores Eletroquímicos (LabSensE), Departamento de Química, Universidade Federal do Paraná (UFPR), CEP 81.531-980 Curitiba, PR, Brazil*

[b] *Campus Paranavaí, Instituto Federal do Paraná, 87703-536 Paranavaí, PR, Brazil*

[c] *Faculty of Science and Engineering, Manchester Metropolitan University, Chester Street, Manchester M1 5GD, UK*

Microfluidic devices constructed using low cost materials presents as alternative for conventional flow analysis systems because they provide advantages as low consumption of reagents and samples, high speed of analysis, possibility of portability and the easiness of construction and maintenance. Herein, is described for the first time the use of an electrochemical biosensor for phenol detection combined with a very simple and efficient microfluidic device based on commercial textile threads. Taking advantages of capillary phenomena and gravity forces, the solution transportation is promoted without any external forces or injection pump. Screen printed electrodes were modified with carbon nanotubes/gold nanoparticles followed by covalent binding of tyrosinase. After the biosensor electrochemical characterization by cyclic voltammetry technique, the optimization of relevant parameters such as pH, potential of detection and linear range for the biosensor performance was carried out; the system was evaluated for analytical phenol detection presenting limit of detection and limit of quantification 2.94 nmol L−1 and 8.92 nmol L−1 respectively. The proposed system was applied on phenol addition and recovery studies in drinking water, obtaining recoveries rates between 90% and 110%.

1. Introduction

The miniaturization of analytical systems began in the late 1970s, when Terry et al. (Reyes et al., 2002) presented a portable gas chromatograph, which was able to make small separations using thermal conductivity detection. From then on, microfluidic systems have experienced explosive growth since its development also they are known as micro total analysis system (μTAS). These devices have been fabricated using materials such as glass, polymers, hydrogels, paper and other materials (Burns et al., 1998; Neuži et al., 2012; Parolo and Merkoci, 2013).

In the last few years, cotton thread-based devices appear as a promising option to overcome some limitations imposed by paper-based microfluidic analytical devices (μPAD) such as low efficiency of sample delivery, low mechanical strength of wet paper, problems with low surface tension of the sample and the requirement of construction of hydrophobic barriers to delimit microchannels (Desmet et al., 2016; Santhiago and Kubota, 2013). Concerning properties for the use of cotton thread as low cost microfluidic analytical device, some advantages can be cited as liquid flow by capillary forces without external pumping, flexibility, high mechanical strength when wet, low cost, worldwide availability, disposability and not required construction of hydrophobic barriers to design microchannels (Mitchell et al., 2005; Nilghaz et al., 2015, 2013).

Most of the analytical work using cotton-thread devices consists in colorimetric detection which depends on ability of visual discrimination from analyst (Jia et al.; Nilghaz et al., 2015). The combination of cotton-threads and electrochemical detection is relatively new topic in electroanalytical procedures (Agustini et al., 2016). This first work related describes the construction of low cost microfluidic thread-based electroanalytical device (μ-TED) employing graphite electrodes which was used for simultaneous amperometric determination of acetaminophen and diclofenac and a second work describing the optimization of μ-TED devices (Agustini et al., 2017). Ochiai et al. (2017) described μ-TED using multiwalled carbon nanotubes (MWCNTs) modified screen printed electrodes (SPE) for electrochemical determination of estriol hormone using amperometry, obtaining a limit of detection of 5.3×10^{-7} mol L^{-1}.

The research in order to develop new biosensors for phenolic compounds determination has been increased in the last years, since these compounds present potential hazard for aquatic life and human health (Mukherjee et al., 2013); usually appears in the environment via industrial wastes from a plenty of kinds of production such as plastics, dyes, drugs, resins, pesticides, and especially paper and cellulose (Villegas et al., 2016). Therefore, it is considered a priority pollutant by the American Environmental Protection Agency (EPA, 2016) which has established its limit concentration in drinking water as 1.0×10^{-8} mol L^{-1}.

In this present work, we report the first enzymatic biosensor employed as an electrochemical detector combined with μ-TED system. For this, Tyrosinase was covalently immobilized onto multiwalled carbon nanotubes and gold nanoparticles (GNPs/MWCNT) nanocomposite using a disposable carbon screen printed electrode (C-SPE) and the phenol detection was performed in tap water. The SPE provide disposable, planar, low-cost miniaturized size and incorporate the whole electrode system (working, reference and auxiliary) in a single device, which are suitable characteristics for the proposed microfluidic device (Mohamed, 2016). In electroanalysis, more specific for development of new biosensors architecture, gold nanoparticles have been highly employed due to some characteristics such as a good mechanical resistance and electrical properties, high surface area for enzyme immobilization and biocompatibility (Gevaerd et al., 2015; Lan et al., 2017; Vicentini et al., 2016; Vidotti et al., 2011). Tyrosinase (Tyr) is also known as polyphenol oxidase (PPO) or catechol oxidase (Shleev et al., 2005; Yaropolov et al., 1996), catalyzes the oxidation reactions, such as: the hydroxylation of monophenols to o-dihydroxy phenols, and subsequently the oxidation-dihydroxy phenols to o-quinones in the presence of molecular oxygen. The o-quinone can be easily detected by electrochemical techniques such as voltammetry or amperometry (Kochana et al., 2015; Tan et al., 2011).

2. Experimental section

2.1. Reagents

All the chemicals were analytical grade and used as received from Sigma–Aldrich. Multi-walled carbon nanotubes sample (MWCNTs) was purchase from Dropsens (purity of 95%, length 1.5 μm, diameter 10 nm). All solutions were prepared with deionized water (specific resistivity > 18 MΩ cm) obtained with a Millipore Direct-Q3 water purification system.

2.2. Synthesis of GNPs/MWCNT nanocomposite and SPE modification

The nanocomposite (GNPs-MWCNTs) used as platform for *tyrosi- nase* immobilization was synthesised following the procedure fully described in a previous work by Caetano et al. (2017). Briefly, the methodology consists in a biphasic system (water/toluene) where the

reduction of gold precursor $H[AuCl_4]$ by $NaBH_4$ in presence of MWCNTs is performed. As a result, well dispersed gold nanoparticles (7 ±4 nm) onto multiwalled carbon nanotubes were obtained.

Electrode printing process was carried out using the appropriate masks and a microdek 1670RS printer which the steps consisted of the deposition of graphite carbon inks (for working electrode and auxiliary electrode printing), Ag/AgCl (reference electrode) and dielectric ink (Gwent, Liverpool, UK) on a polyester substrate (Rana et al., 2017)

A 1.0 mg mL^{-1} suspension of GNPs-MWCNTs in isopropyl alcohol containing 0.05% (w/v) of Nafion® was subjected to ultrasonication for 20 min. The chemically modified electrode was prepared by drop casting using 3.0 µL of suspension onto the C-SPE (geometrical arean= 0.07 mm^2) and let dry at room temperature for 1 h. Cyclic Voltammograms were recorded using a conventional reference electrode Ag/AgCl (KCl 3.0 mol L^{-1}).

Tyrosinase immobilization

Working electrode containing GNPs-MWCNTs was chemically modified with cystamine (CYS) and glutaraldehyde (GA) to link the Tyr covalently. Firstly, 20 µL of 50 mmol L^{-1} CYS solution was casted onto the electrode surface, and the solvent was evaporated at room temperature for 1 h, and then rinsed with 0.1 mol L^{-1} phosphate buffer solution (PB, pH 6.5). Subsequently, 20 µL of 2.5% (v/v) GA solution was casted onto surface of GNPs-MWCNTs modified electrode and the solvent was evaporated at room temperature for 1 h. The electrode was washed with 0.1 mol L^{-1} PB solution (pH 6.5). Finally, 20 µL of a solution containing 100 units of Tyr (5 KU mL^{-1} in PB solution 0.05 mol L^{-1}, pH 6.5) was casted onto the electrode surface and the solvent was evaporated at room temperature overnight. Biossensor (Tyr-GNPs-MWCNTs/SPE) was washed with with 0.1 mol L^{-1} PB solution (pH 6.5) and kept at −4 °C.

2.3. Construction of the thread-based electroanalytical device (µTED) and Electrochemical measurements

The material used as substrate was ABS (Acrylonitrile-butadiene- styrene) polymer using a GTMax3D printer - Graber i3 model (Americana – SP, Brazil). The proposed device (Fig. 1) was developed by printing a plastic support using a 3D printer (25 mm of wideness, 6.5 mm of thickness and length 90, 60 and 30 mm) were used as the substrate for assembly of the µTED. The scheme presented in Fig. 1 shows the device structure. The device construction steps consists in (i) placement of two pieces of double sided scotch tape near the inlet and outlet reservoirs; (ii) accommodation of Tyr-GNPs-MWCNTs/SPE on the double-sided tape next to the outlet reservoir; (iii) fixation of arrangement of microchannels which are formed hydrophilic threads (9 parallel threads without twisting) throughout the device, from the inlet reservoir to the outlet reservoir; (iv) placement of two pieces of double sided tape on the ends of the hydrophilic gauze. Detection zone was covered by pieces of cotton thread in order to maintain all electrodes immersed in solution during measurements.

2.4. Transmission electron microscopy, Scanning Electron Microscopy, X-ray diffraction and electrochemical analysis

The size and distribution of the GNPs were determined by means of transmission electron microscopy (TEM) using a JEOL JEM 1200 operated at 120 kV. The samples were prepared by dropping the nanohybrid suspension standard hole cupper grids covered by a thin parlodium film. Scanning electron microscopy (SEM) analysis were carried out in a TESCAN Vega 3 equipment, operated at 120 kV. X-ray diffraction measurements were carried out in a Shimadzu XRD−3A

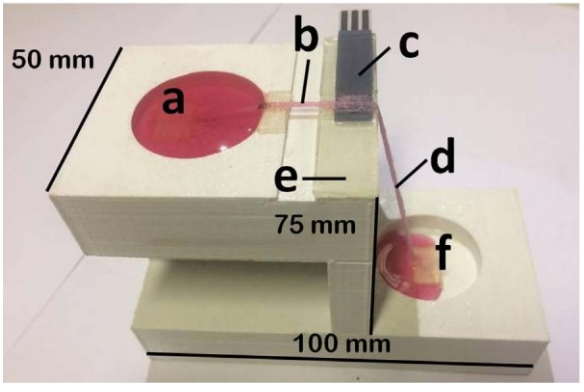

Fig. 1. Dimensions and constituents parts μ-TED a) Inlet reservoir b) injection zone c) SPE (Electrochemical detection zone) d) Hydrophilic textile thread e) Adhesive tape f) outlet reservoir. To demonstrate the solution flux on threads, a food coloring was employed.

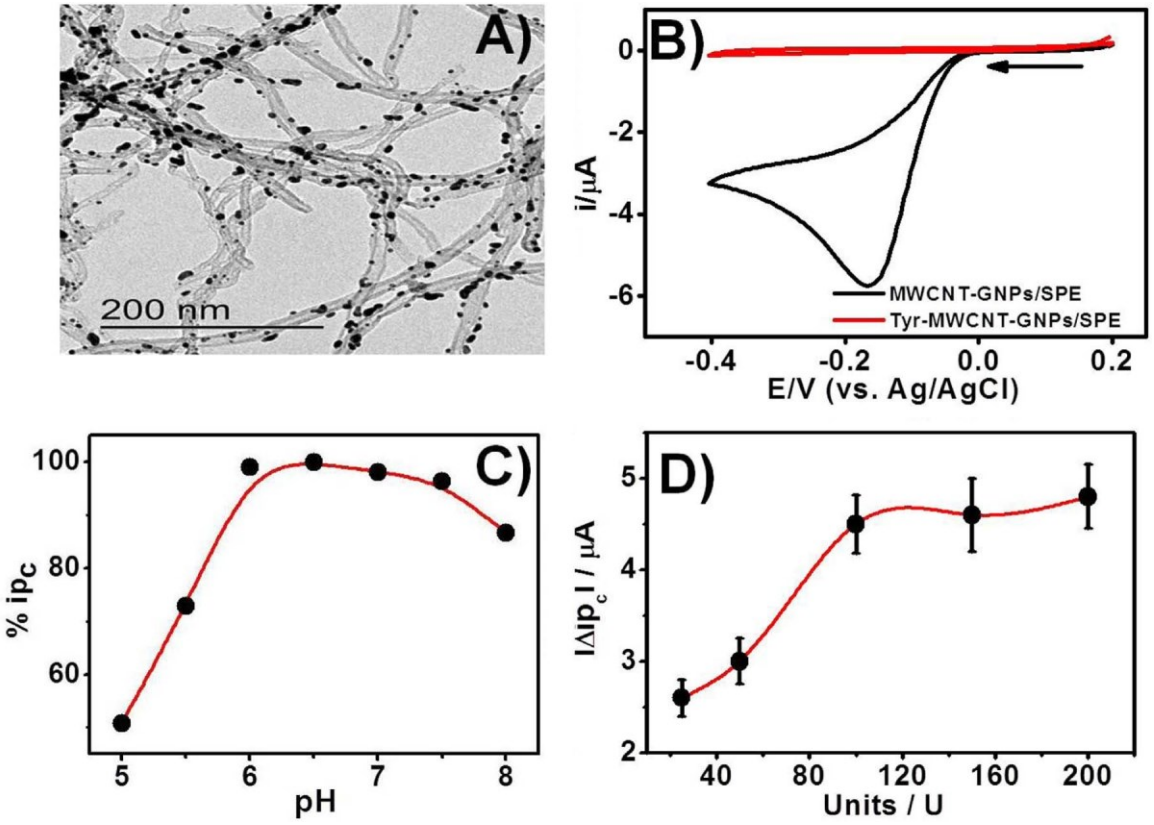

Fig. 2. A) TEM image of MWCNT-GNPs nanocomposite B) Comparative cyclic voltamogramms of CNT-GNPs before and after Tyr immobilization procedure. Experimental conditions: PB solution 0.1 mol L^{-1} (pH 6.5) containing phenol 100 μmol L^{-1}, v = 5 mV s^{-1}, potential ranging from 0.2 to −0.4 V *vs* Ag/AgCl C) CVs relative responses of cathodic peak current versus pH of electrolyte solution using PB solution 0.1 mol L^{-1} and phenol 100 μmol L^{-1} as substrate. D) Cathodic peak current response for different concentrations of Tyr added onto MWCNT-GNPs/SPE electrodes using PB solution 0.1 mol L^{-1} (pH 6.5) and phenol 100 μmol L^{-1} as substrate.

2.5. Transmission electron microscopy, Scanning Electron Microscopy, X-ray diffraction and electrochemical analysis

The size and distribution of the GNPs were determined by means of transmission electron microscopy (TEM) using a JEOL JEM 1200 operated at 120 kV. The samples were prepared by dropping the nanohybrid suspension standard hole cupper grids covered by a thin parlodium film. Scanning electron microscopy (SEM) analysis were carried out in a TESCAN Vega 3 equipment, operated at 120 kV. X-ray diffraction measurements were carried out in a Shimadzu XRD−3A diffractometer using Cu K α radiation, with voltage and current of 40 kV and 40 mA respectively, 0.02 scan rate (in 2 θ). Powder silicon reflections were used for 2θ calibration. TGA were done on a SDT Q600 equipment (TA Instruments) under air (100 mL min^{-1}) and at heating rate of 5 °C min^{-1}, using an alumina pan holder.

All electrochemical measurements were conducted with the potentiostat/galvanostat (μAutolab type III; Metrohm Autolab B.V., Utrecht, the Netherlands). Supporting electrolyte solution was 0.10 mol L^{-1} PB pH 6.5.

3. Results and discussion

3.1. Biosensor characterization

In order to confirm nanocomposite structure, TEM analysis was carried out to evaluate the dispersion degree of GNPs on MWCNTs. As can be seen in Fig. 2A an uniform, well-distributed and non-agglomerated dispersion of gold nanoparticles composed by a mixture of spherical and spherical condensed-like nanoparticles was yielded on the MWCNT surface. Comparative SEM images (supplementary section, Fig. S1-A,B) were obtained at 25,000 X where the SPE surface presents a surface modification after chemical incorporation of GNPs/MWCNTs. X-ray diffraction analysis (Fig. S1-C) presents the well- defined peaks at $2\theta = 37.9°, 44.2°$, and $64.4°$ characteristics of gold with a fcc structure (JCPDS 04–0784).

Electrochemical behaviour of $[Fe(CN)_6]^{3-}$ step by step modification of the SPE in 1.0 mmol L^{-1} $[Fe(CN)_6]^{3-}$ (pH 6.5) were investigated. The SPE showed a well-defined redox wave (Supplementary section, Fig. 2) corresponding to the redox reaction of ferricyanide ions. GNP-MWCNTs provide slight current increase due to high surface area of nanocomposite. Tyr loading onto electrode surface results in a current decrease provided by blocking effect provided by protein layer. Enzyme immobilization and maintenance of catalytic properties were tested by comparative electrochemical behaviour between GNPs-MWCNTs elec- trodes before and after Tyr addition protocol described at item 2.3.

Preliminary cyclic voltammograms were recorded in 0.1 mol L^{-1} PB solution (pH 6.5) as support electrolyte containing 1.0×10^{-4} mol L^{-1} phenol, the voltage was swept from 0.2 V to - 0.4 V as can be seen at Fig. 2B, Tyr-GNPs-MWCNTs/SPE presented an intense current at E_{pc} = − 168 mV *vs* Ag/AgCl/ KCl 3.0 mol L^{-1}. In the same conditions, GNPs-MWCNTs/SPE not presented a reduction peak. Tyr catalyzes the oxidation of phenol to o-quinone in presence of molecular oxygen (Yaropolov et al., 1996). Therefore, o-quinone is electrochemically reduced regenerating the catechol at the electrode surface and increas- ing the analytical signal (Kochana et al., 2015; Vicentini et al., 2016). Enzymes have their catalytic activity strongly affected by pH. Cathodic peak currents were studied over the range 5.0–8.0 and the highest current values was found to pH 6.5 as can be seen at Fig. 2C, which is in agreement with copper containing enzymes structure (T2 and T3 types). Normally they present maximum catalytic activity at pH 6.5–7.0 which is related to histidine protonation nearby catalytic copper center (*his* 287, pKa ~ 6.5) (Jacobson et al., 2007).

Gold nanoparticles provide several sites for enzyme immobilization and Tyr concentration onto SPE is directly related to obtained signal. In order to find the best relation nanocomposite/enzyme, for all experiments an aliquot of 3.0 μL GNPs-MWCNTs dispersion (1.0 mg mL^{-1}) was fixed and the volume of enzyme solution casted onto GNPs-MWCNTs/SPE was evaluated. Fig. 2D shows the cathodic peak current response founded by CV technique in presence of phenol 100 μmol L^{-1}. Values above 100 U present stabilization of ip_c without significant variation, indicating saturation of immobilization sites by Tyr on MWCNT-GNPs nanocomposites. The enzyme amount was fixed at 100 U which correspond of 20 μL Tyr 5 KU mL^{-1} stock solution.

3.2. Development and application of analytical method using μTED with screen-printed carbon electrodes

Since Tyr-GNPs-MWCNTs/SPE exhibits stable electrochemical response toward phenol, the effectiveness of proposed μ-TED device was evaluated. Fig. 2A shows the typical behavior of 100 μmol L^{-1} phenol in PB pH 6.5 as both support electrolyte and carrier solution through amperometry at - 300 mV, a well-defined signal was observed. In absence of phenol a stable baseline without significant variations was verified in all experiments realized. Right after phenol addition, the current decreases around 300 μA, returning to the previous baseline after 60 s. The signal obtained can be attributed to the combination of physical and chemical processes: i) when phenol is added on the thread channels, it is moved to the electrode zone quickly by capillary forces ii) at the electrode zone, Tyr converts phenol to o-quinone followed by electrochemical reduction generating current decrease iii) after full passage of phenol onto the electrode zone, the current signal returns to

baseline.

The sensitivity of chronoamperometry measurements is dependent on the applied potential at working electrode. Thus, the phenol detection potentials were tested at potentials from −100 to −500 mV using a 100 μmol L^{-1} solution of phenol and results are shown in Fig. 3B. Current values were presented as relative intensity (%) in order to facilitate the observations and tendencies. As can be seen, the variation of applied potential reaches the higher current intensity at −300 mV. At more negative values of potential (−400 mV and −500 mV), the Δ_{ipc} presents smaller values and a pronounced capaci- tive contribution on resultant current was observed. Based on best relation signal/noise a potential of −300 mV was chosen as optimum potential for phenol detection.

Electrochemical characterization of Tyr-GNPs-MWCNTs/SPE by CV was carried out using an external reference electrode (RE) aiming to compare the potential of o-quinone reduction. Concerning phenol electrochemical detection, the potential variation presented was +180 mV in relation to the RE. As a result, the reaction occurs at −300 mV in relation to the pseudo-RE, is shifted to −120 mV *vs*. Ag/AgCl/KCl 3.0 mol L^{-1}. This variation is in agreement with the poten- tials described in the literature, where the o-quinone reduction occurs between 100 and −100 mV *vs*. Ag/AgCl/KCl 3.0 mol L^{-1} (Hervás Pérez et al., 2006; Sethuraman et al., 2016; Tan et al., 2010; Zhang et al., 2009). After optimizing the relevant parameters on μ-TED response, successive additions of 2.0 μL of phenol from 10 nmol L^{-1} to 800 nmol L^{-1} were carried out in order to verify the fouling tendency of the μTED, the phenol concentration was varied from the minimal to the maximal concentration value and in sequence returning back to the minimal concentration. As can be seen in Fig. 4A, no fouling tendency was observed, probably due to the use of continuous flow support electrolyte over the electrode surface, cleaning of the Tyr-GNPs-MWCNTs/SPE surface after each injection. Monitoring the solution mass in outlet reservoir and assuming the density of solution to be 0.998 g mL^{-1} at 20 °C (LIDE, 2004) the transported solution volume increased linearly over time (R = 0.991 = 0.991) with a flow rate stable of 0.44 μL s^{-1} without significant oscillations for at least 1 h.

The reduction peak currents were found proportional to the concentrations of phenol over the range from 10.0 to 200 nmol L^{-1} presenting curve equation $|\Delta_{ipc}|$ / nA = 1.63 + 0.131C_{phenol} / μmol L^{-1} with a correlation coefficient of 0.996, limit of detection (LOD) was estimated to be 2.94 nmol L^{-1} (LOD = 3.3 δ/LOD = 3.3 δ/S where δ is the standard deviation of blank samples, S is detection sensitivity (slope of calibration curve where δ is the standard deviation of blank samples, LOD = 3.3 δ/S where δ is the standard deviation of blank samples, S is detection sensitivity (slope of calibration curve is detection sensitivity (slope of calibration curve)) and limit of quantification (LOQ = 10 δ/S) was estimated as 8.92 nmol L^{-1}. The values of standard deviation of repeatability was found to be 7.3% (n = 5) for five successive injections at the same device and 12% (n = 5) for reproducibility tests where five different devices were constructed

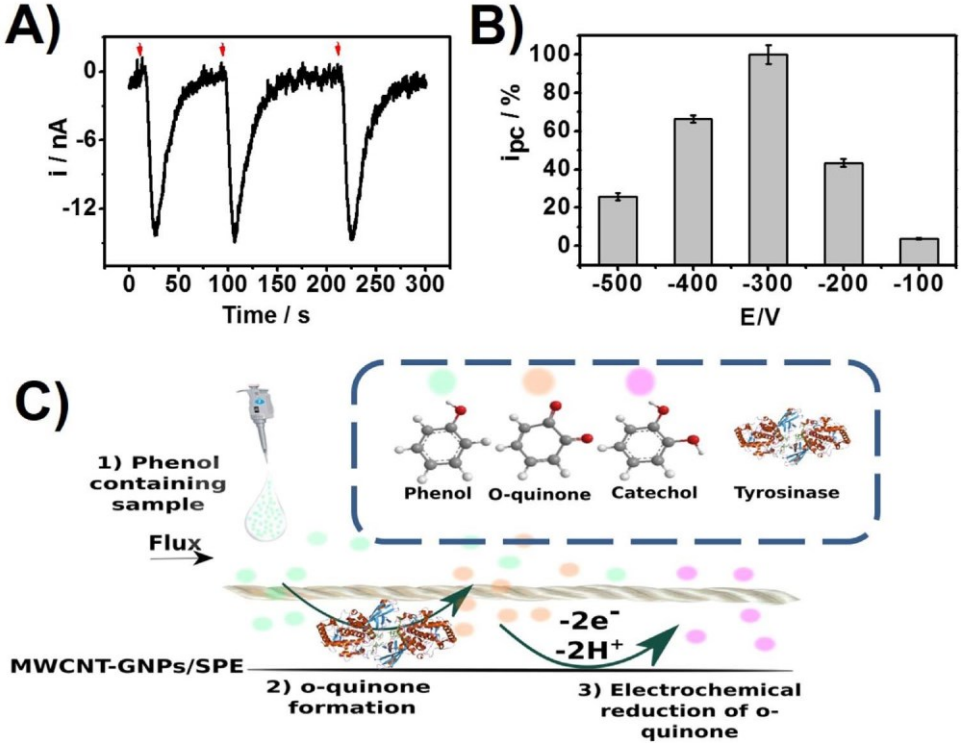

Fig. 3. A) Chronoamperometric response of μ-TED Potential recorded at −300 mV *vs* Ag for injections of 2.0 μL B) Variation of amperometric response and potential of detection from
−100 mV to −500 mV. C) Schematic diagram of proposed μ-TED system for phenol detection indicating the steps: sample injection (1), o-quinone formation (2) and electrochemical reduction (3). All experiments were carried out using PB solution 0.1

mol L^{-1} (pH 6.5) as support electrolyte and phenol 120 nmol L^{-1} as substrate.

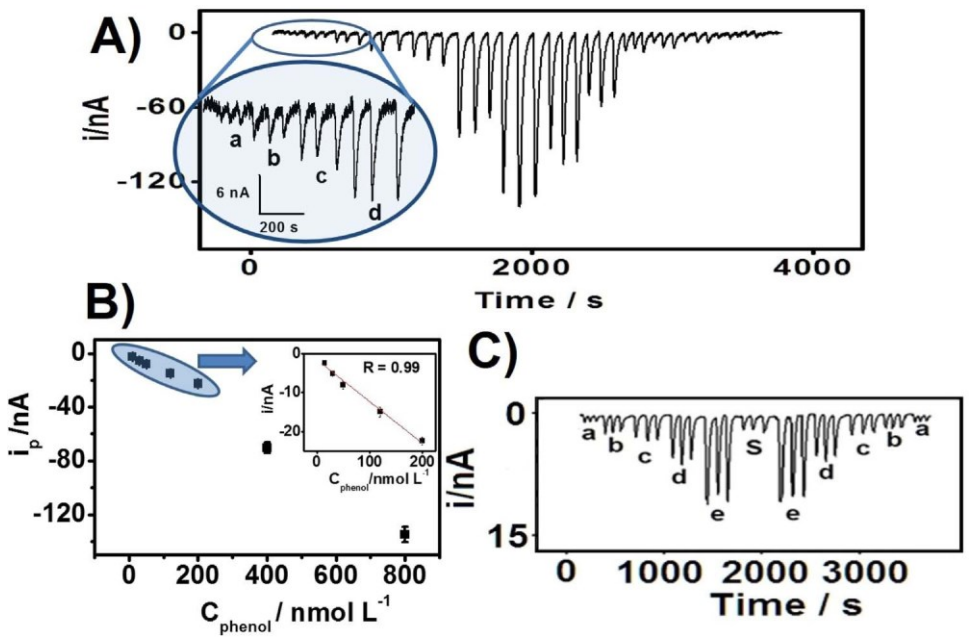

Fig. 4. A) Successive amperometric response in μ-TED obtained for injections of 2.0 μL of phenol standard solutions aliquots using PB solution 0.1 mol L^{-1} (pH 6.5), varying over range 10.0–800 nmol L^{-1} Inset: (a) 10; (b) 30; (c) 50; and (d) 120 nmol L^{-1}, with a flow rate of 0.44 μL s^{-1} B) calibration curve from 10 nmol L^{-1} – 800 nmol L^{-1} (inset: dynamic linear range from 10 to 200 nmol L^{-1}) and C) Successive amperometric responses obtained for injections of 2.0 μL of phenol standard solutions aliquots (a) 10; (b) 20; (c) 40; (d) 80; (e) 100 nmol L^{-1}; and phenol spiked tap water (S) 20 nmol L^{-1}, varying over a range, flow rate of 0.44 μL s^{-1}, applied potential: −300 mV.

(Supplementary section, Fig. S3). The analytical frequency for successive additions of 50 nmol L^{-1} of phenol was 54 injections per hour.

As previously reported, some molecules can promote the enzymatic deactivation acting as both substrate and inhibitor (Haghbeen et al., constant of Michaelis-Menten (K_M^{app}) provides important information on the catalytic activity and affinity between the immobilized enzyme and the substrate. These values can be obtained by Lineweaver-Burk's Eq. Such behavior is called suicide effect and phenol can present such effect on Tyr catalytic activity. Some authors indicate the loss of catalytic activity occurs in diphenolase cycle leading to the irreversible reduction of copper causing enzyme deactivation (Muñoz-Muñoz et al., 2010). The biosensor retained the 95% of the initial signal during 7 days and then a fast fall in the response (descent of 70% in the signal) was observed. In Table 1 are described some comparative analytical parameters in the determination of phenol via electrochemistry using Tyr-based biosensors reported in literature. The values for the present work are satisfactory, analysing the limits of detection and linear range, presenting, an intermediate sensitivity was achieved in relation to the others biosensors. The apparent kinetic C_{Phenol} plot and for the Tyr-MWCNT- GNPs/SPE was 4.9 μmol L^{-1}, in concordance with other Tyr-based electrochemical biosensors (Campuzano et al., 2003; Lu et al., 2010; Tsai and Chiu, 2007). The cost of each device was estimated to be US$3.70 (Supplementary section, Table S1) where 73% of such value corresponds to modified SPE (GNPs-MWCNTs and Tyr), hydrophilic threads and double-sided tape. Due to the quantity of both nanocomposite (3 μg) and enzyme (100 U) required to SPE modification, the costs of production become the μ-TED a competitive device for its purpose (Table 2)

Table 1
Analytical parameters for electrochemical Tyr-based biosensors towards Phenol detection.

Electrode	Technique	LOD (nM)	Sens. (μA mM^{-1})	Linear Range (μM)	Refs.
Graphite-EDC– NHS–Tyr	FIA- Amp	3	321	0.01–5.0	(Ortega et al., 1993)
Au –MPA-Tyr	FIA–Amp	0.8	1300	0.2–200	(Campuzano et al., 2003)
GCE–EDS– NHS–Tyr	FIA–Amp	260	8	0.5–30	(Peña et al., 2001)
Au-HA-Chit-Tyr	Amp	10	1.77	0.07–5.0	(Lu et al., 2010)
GCE-CNTs– nafion–Tyr	Amp	130	303	1–19	(Tsai and Chiu, 2007)

BDD-AuNP-Tyr	SWV	70	1800	0.10–11	(Janegitz et al., 2012)
GCE-Graphene–Aminoac-Tyr	Amp	0.35	4.08	0.001–21	(Qu et al., 2013)
This work	μ-TED Amp	2.94	131	0.01–0.2	–

EDC - N-Ethyl-N′-(3-dimethylaminopropyl)carbodiimide / NHS - N-Hydroxysuccinimide / MPA −3-Mercaptopropionic acid / GCE – Glassy Carbon Electrode / HA – hydroxyapatite / Chit –

chitosan / BDD – Boron-doped Diamond Electrode / Aminoac – Aminoacid modified / FIA – Flux Injection Analysis / Amp – Amperometry / SWV – Square Wave Voltammetry /.

Table 2
phenol recovery tests in tap water.

Added (nmol L^{-1})	Recovered	Recovered (%)
20	22 ± 6	110 ± 30
60	58 ± 9	96 ± 10
100	89 ± 13	89 ± 13

3.3. Application of μ-*TED in tap water samples*

The practical application of μ-TED was tested by recovery tests carried out to evaluate the accuracy of the proposed method. The tap water samples were provided by Sanitation Company of Paraná, at Chemistry Department of Federal University of Paraná, Curitiba/PR-Brazil. In Fig. 4B are shown the profile addition of standard concentrations of phenol (a–e), followed by spiked tap water 20 nmol L^{-1} phenol (S) addition and then, decreasing standard phenol concentrations (e–a). The presence of tap water components does not affect the electrochemical μ-TED response.

The addition and recovery studies were performed at 3 levels (20, 60 and 100 nmol L^{-1}, the recovery obtained range from 89% to 110%. According to Sanitation Company (SANEPAR, 2016) the main components found in provided tap water are: fluorides (0.7 ppm – 3.68×10^{-5} mol L^{-1}), residual chlorine (1.2 ppm – 1.69×10^{-5} mol L^{-1}), aluminum (0.08 ppm – 2.95×10^{-6} mol L^{-1}), iron and manganese (0.05 ppm – 8.95×10^{-7} mol L^{-1}) and microcystin (1 ppb). Thus, the results obtained for the determination of phenol in enriched samples showed good agreement, validating the μ-TED to conduct for phenol determination in tap water samples.

4. Conclusions

In this work, electrochemical biosensor combined with textile threads were used to construct a low cost microfluidic device for phenol detection. Tyrosinase was loaded onto gold nanoparticles- carbon nanotubes nanocomposite. These materials were selected considering its biocompatibility. The results showed ease of construction and application for phenol detection presenting good linear range (10–200 nmol L^{-1}), low limit of detection (2.91 nmol L^{-1}), good sensitivity (131 nA μmol L^{-1}) when compared to other phenol electrochemical sensors, small variation between the injections (7,3%) and the measurements with different devices (12%). The analytical performance of proposed device was evaluated by recovery studies in tap water and the range of 89–100% was found. Thus, the analyses carried out in μTED allows the realization of phenol in a simple, fast, cheap and reliable assay, in addition to a good analytical performance.

References

Agustini, D., Bergamini, M.F., Marcolino-Junior, L.H., 2016. Low cost microfluidic device based on cotton threads for electroanalytical application. Lab Chip 16 (2), 345–352.

Agustini, D., Bergamini, M.F., Marcolino-Junior, L.H., 2017. Characterization and optimization of low cost microfluidic thread based electroanalytical device for micro flow injection analysis. Anal. Chim. Acta 951, 108–115.

Burns, M.A., Johnson, B.N., Brahmasandra, S.N., Handique, K., Webster, J.R., Krishnan, M., Sammarco, T.S., Man, P.M., Jones, D., Heldsinger, D., Mastrangelo, C.H., Burke, D.T., 1998. An integrated nanoliter DNA analysis device. Science 282 (5388), 484–487.

Caetano, F.R., Felippe, L.B., Zarbin, A.J.G., Bergamini, M.F., Marcolino-Junior, L.H., 2017. Gold nanoparticles supported on multi-walled carbon nanotubes produced by biphasic modified method and dopamine sensing application. Sens. Actuators B: Chem. 243, 43–50.

Campuzano, S., Serra, B., Pedrero, Ma, de Villena, F.J.M., Pingarrón, J.M., 2003. Amperometric flow-injection determination of phenolic compounds at self- assembled monolayer-based tyrosinase biosensors. Anal. Chim. Acta 494 (1), 187–197.
Desmet, C., Marquette, C.A., Blum, L.J., Doumèche, B., 2016. Paper electrodes for bioelectrochemistry: biosensors and biofuel cells. Biosens. Bioelectron. 76, 145–163.
EPA, 2016. Toxics Release Inventory Program. EPA.
Gevaerd, A., Caetano, F.R., Oliveira, P.R., Zarbin, A.J.G., Bergamini, M.F., Marcolino- Junior, L.H., 2015. Thiol-capped gold nanoparticles: influence of capping amount on electrochemical behavior and potential application as voltammetric sensor for diltiazem. Sens. Actuators B: Chem. 220, 673–678.
Haghbeen, K., Saboury, A.A., Karbassi, F., 2004. Substrate share in the suicide inactivation of mushroom tyrosinase. Biochim. Biophys. Acta - Gen. Subj. 1675 (1– 3), 139–146.
Hervás Pérez, J.P., Sánchez-Paniagua López, M., López-Cabarcos, E., López-Ruiz, B., 2006. Amperometric tyrosinase biosensor based on polyacrylamide microgels.
Biosens. Bioelectron. 22 (3), 429–439.
Jacobson, F., Pistorius, A., Farkas, D., De Grip, W., Hansson, Ö., Sjölin, L., Neutze, R., 2007. pH dependence of copper geometry, reduction potential, and nitrite affinity in nitrite reductase. J. Biol. Chem. 282 (9), 6347–6355.
Janegitz, B.C., Medeiros, R.A., Rocha-Filho, R.C., Fatibello-Filho, O., 2012. Direct electrochemistry of tyrosinase and biosensing for phenol based on gold nanoparticles electrodeposited on a boron-doped diamond electrode. Diam. Relat. Mater. 25, 128–133.
Jia, X., Song, T., Liu, Y., Meng, L., Mao, X., An immunochromatographic assay for carcinoembryonic antigen on cotton thread using a composite of carbon nanotubes and gold nanoparticles as reporters. Anal. Chim. Acta.
Kochana, J., Wapiennik, K., Kozak, J., Knihnicki, P., Pollap, A., Woźniakiewicz, M., Nowak, J., Kościelniak, P., 2015. Tyrosinase-based biosensor for determination of bisphenol A in a flow-batch system. Talanta 144, 163–170.
Lan, L., Yao, Y., Ping, J., Ying, Y., 2017. Recent advances in nanomaterial-based biosensors for antibiotics detection.
Biosens. Bioelectron. 91, 504–514.
LIDE, D.R., 2004. Handbook of Chemistry and Physics 84 ed.
Lu, L., Zhang, L., Zhang, X., Huan, S., Shen, G., Yu, R., 2010. A novel tyrosinase biosensor based on hydroxyapatite–chitosan nanocomposite for the detection of phenolic compounds. Anal. Chim. Acta 665 (2), 146–151.
Mitchell, R., Carr, C., Parfitt, M., Vickerman, J., Jones, C., 2005. Surface chemical analysis of raw cotton fibres and associated materials. Cellulose 12 (6), 629–639.
Mohamed, H.M., 2016. Screen-printed disposable electrodes: pharmaceutical applications and recent developments. Trends Anal. Chem. 82, 1–11.
Mukherjee, S., Basak, B., Bhunia, B., Dey, A., Mondal, B., 2013. Potential use of polyphenol oxidases (PPO) in the bioremediation of phenolic contaminants containing industrial wastewater. Rev. Environ. Sci. Bio/Technol. 12 (1), 61–73.
Muñoz-Muñoz, J.L., Garcia-Molina, F., Varon, R., Garcia-Ruíz, P.A., Tudela, J., Garcia- Cánovas, F., Rodríguez-López, J.N., 2010. Suicide inactivation of the diphenolase and monophenolase activities of tyrosinase. IUBMB Life 62 (7), 539–547.
Neuži, P., Giselbrecht, S., Länge, K., Huang, T.J., Manz, A., 2012. Revisiting lab-on-a- chip technology for drug discovery. Nat. Rev. Drug Discov. 11 (8), 620–632.
Nilghaz, A., Bagherbaigi, S., Lam, C., Mousavi, S., Corcoles, E., Wicaksono, D., 2015. Multiple semi-quantitative colorimetric assays in compact embeddable microfluidic cloth-based analytical device (mu CAD) for effective point-of-care diagnostic. Microfluid. Nanofluidics 19 (2), 317–333.
Nilghaz, A., Ballerini, D., Shen, W., 2013. Exploration of microfluidic devices based on multi-filament threads and textiles: a review. Biomicrofluidics 7, 5.
Ochiai, L.M., Agustini, D., Figueiredo-Filho, L.C.S., Banks, C.E., Marcolino-Junior, L.H., Bergamini, M.F., 2017.
Electroanalytical thread-device for estriol determination using screen-printed carbon electrodes modified with carbon nanotubes. Sens.
Actuators B: Chem. 241, 978–984.
Ortega, F., Domínguez, E., Jönsson-Pettersson, G., Gorton, L., 1993. Biosensors and Flow Injection Analysis Amperometric biosensor for the determination of phenolic compounds using a tyrosinase graphite electrode in a flow injection system. J. Biotechnol. 31 (3), 289–300.
Parolo, C., Merkoci, A., 2013. Paper-based nanobiosensors for diagnostics. Chem. Soc.
Rev. 42 (2), 450–457.
Peña, N., Reviejo, A.J., Pingarrón, J.M., 2001. Detection of phenolic compounds in flow systems based on tyrosinase-modified reticulated vitreous carbon electrodes. Talanta 55 (1), 179–187.
Qu, Y., Ma, M., Wang, Z., Zhan, G., Li, B., Wang, X., Fang, H., Zhang, H., Li, C., 2013.
Sensitive amperometric biosensor for phenolic compounds based on graphene–silk peptide/tyrosinase composite nanointerface. Biosens. Bioelectron. 44, 85–88.
Rana, S., Mittal, S.K., Singh, N., Singh, J., Banks, C.E., 2017. Schiff base modified screen printed electrode for selective determination

of aluminium(III) at trace level. Sens. Actuators B: Chem. 239, 17–27.
Reyes, D.R., Iossifidis, D., Auroux, P.-A., Manz, A., 2002. Micro total analysis systems. 1. Introduction, theory, and technology. Anal. Chem. 74 (12), 2623–2636.
SANEPAR, 2016. Registros sobre a composição da água distribuida.
Santhiago, M., Kubota, L.T., 2013. A new approach for paper-based analytical devices with electrochemical detection based on graphite pencil electrodes. Sens. Actuators B: Chem. 177, 224–230.
Sethuraman, V., Muthuraja, P., Anandha Raj, J., Manisankar, P., 2016. A highly sensitive electrochemical biosensor for catechol using conducting polymer reduced graphene oxide–metal oxide enzyme modified electrode. Biosens. Bioelectron. 84, 112–119.
Shleev, S., Tkac, J., Christenson, A., Ruzgas, T., Yaropolov, A.I., Whittaker, J.W., Gorton, L., 2005. Direct electron transfer between copper-containing proteins and electrodes. Biosens. Bioelectron. 20 (12), 2517–2554.
Tan, Y., Guo, X., Zhang, J., Kan, J., 2010. Amperometric catechol biosensor based on

polyaniline–polyphenol oxidase. Biosens. Bioelectron. 25 (7), 1681–1687.
Tan, Y., Kan, J., Li, S., 2011. Amperometric biosensor for catechol using electrochemical template process. Sens. Actuators B: Chem. 152 (2), 285–291.
Tsai, Y.-C., Chiu, C.-C., 2007. Amperometric biosensors based on multiwalled carbon nanotube-Nafion-tyrosinase nanobiocomposites for the determination of phenolic compounds. Sens. Actuators B: Chem. 125 (1), 10–16.
Vicentini, F.C., Garcia, L.L.C., Figueiredo-Filho, L.C.S., Janegitz, B.C., Fatibello-Filho, O., 2016. A biosensor based on gold nanoparticles, dihexadecylphosphate, and tyrosinase for the determination of catechol in natural water. Enzyme Microb. Technol. 84, 17–23.
Vidotti, M., Carvalhal, R.F., Mendes, R.K., Ferreira, D.C.M., Kubota, L.T., 2011.

Biosensors based on gold nanostructures. J. Braz. Chem. Soc. 22, 3–20.
Villegas, L.G.C., Mashhadi, N., Chen, M., Mukherjee, D., Taylor, K.E., Biswas, N., 2016. A short review of techniques for phenol removal from wastewater. Curr. Pollut. Rep., 1–11.
Yaropolov, A.I., Kharybin, A.N., Emnéus, J., Marko-Varga, G., Gorton, L., 1996. Electrochemical properties of some copper-containing oxidases. Bioelectrochem. Bioenerg. 40 (1), 49–57.
Zhang, J., Lei, J., Liu, Y., Zhao, J., Ju, H., 2009. Highly sensitive amperometric biosensors for phenols based on polyaniline–ionic liquid–carbon nanofiber composite. Biosens. Bioelectron. 24 (7), 1858–1863.